Brazil Current surface circulation and energetics observed from drifting buoys

Leopoldo R. Oliveira,[1] Alberto R. Piola,[2] Mauricio M. Mata,[1] and Ivan D. Soares[1]

Received 2 May 2008; revised 29 May 2009; accepted 9 July 2009; published 7 October 2009.

[1] The southwestern Atlantic mean surface circulation, its associated variability and energetics are studied through the analysis of 13 years of surface drifter data binned onto a 0.5° × 0.5° grid. Special attention is given to the following three main regional features of the domain: the Brazil Current, the Malvinas Current, and the Brazil-Malvinas Confluence. For the western boundary currents, the mean field reveals velocities larger than 45 cm s^{-1}, associated with high levels of variability (standard deviation of more than 15 cm s^{-1}), while the highest values of standard deviation are found in the Brazil-Malvinas Confluence (>25 cm s^{-1}). Conversely, over most of the domain the mean velocities found (20–30 cm s^{-1}) and associated standard deviations (<15 cm s^{-1}) are generally lower. High values of kinetic energy of the mean flow per unit mass (265–1000 cm^2 s^{-2}) are estimated in the western boundary currents and their extensions. Eddy kinetic energy along the main jet of the western boundary currents is generally lower than the kinetic energy of the mean flow, except for some areas along the Brazil Current path. In contrast, the Brazil-Malvinas Confluence reveals eddy kinetic energy levels comparable or larger (~2500 cm^2 s^{-2}) than the mean kinetic energy. Away from the boundary, most of the kinetic energy of the surface circulation is in the eddy field. Furthermore, the analysis of the kinetic energy conversion term suggests the presence of barotropic instabilities along the Brazil Current. Over most of the Brazil Current core, the kinetic energy conversion term points from the mean to eddy kinetic energy.

Citation: Oliveira, L. R., A. R. Piola, M. M. Mata, and I. D. Soares (2009), Brazil Current surface circulation and energetics observed from drifting buoys, *J. Geophys. Res.*, *114*, C10006, doi:10.1029/2008JC004900.

1. Introduction

[2] The usable energy in the ocean is mainly contained in the form of kinetic energy, available gravitational potential energy and available internal energy. Among those, the importance of eddy kinetic energy to the large-scale ocean circulation and its role in the formation of midocean eddies has been highlighted by several studies [e.g., *Gill et al.*, 1974; *Dewar and Bane*, 1989; *Phillips and Rintoul*, 2000].

[3] An accurate estimate of the eddy kinetic energy (EKE) is instrumental to calculate the EKE budget, thus leading to reliable estimates of the barotropic conversion processes present in a given ocean area [e.g., *Pedlosky*, 1987]. Similarly, estimates of the eddy potential energy (EPE) budget are necessary for estimating the baroclinic conversion [*Oort et al.*, 1994]. The relative magnitude between the baroclinic and barotropic conversion terms indicates the dominant type of dynamic instabilities (i.e., baroclinic or/and barotropic) of the mean flow, thus helping to identify dynamical processes responsible for the variability observed in a given region [e.g., *Charney*, 1947; *Pedlosky*, 1963, 1964; *Cronin and Watts*, 1996; *Tisch and Ramp*, 1997].

[4] The interaction between the transient eddies and the mean flow of the large-scale gyres is an important component of the energy balance of the oceans. This is particularly relevant near areas where the strong western boundary currents (WBC) separate from the continental margin. In those regions, intense mesoscale activity is frequently observed leading to high levels of eddy energy when compared to most of the remaining areas of the world ocean [e.g., *Olson*, 1991; *Tomczak and Godfrey*, 1994].

[5] Most studies of eddy mean flow interactions near strong WBCs are concentrated in the northern hemisphere [e.g., *Brooks and Niiler*, 1977; *Szabo and Weatherly*, 1979; *Rossby*, 1987; *Dewar and Bane*, 1989; *Hall*, 1991; *Cronin and Watts*, 1996; *Lee and Niiler*, 2005], while few studies have made initial evaluations of the energy conversion terms in the southern hemisphere WBC (Agulhas and East Australian Current) with the aid of numerical models and satellite data [e.g., *Biastoch and Krauss*, 1999; *Mata et al.*, 2006].

[6] Despite its recognized importance to ocean circulation and climate, the energetics of the southwestern Atlantic WBCs is poorly known. In this region, the relatively warm and saline poleward flow of the Brazil Current (BC), which is the western limb of the South Atlantic subtropical gyre, meets the relatively cold, fresh Malvinas Current (MC). The

[1]Instituto de Oceanografia-Laboratório de Estudos dos Oceanos e Clima, Universidade Federal do Rio Grande, Rio Grande, Brazil.

[2]Servicio de Hidrografía Naval, Departamento Oceanografía and Facultad de Ciencias Exactas y Naturales, Departamento Ciencias de la Atmósfera y los Océanos, Universidad de Buenos Aires, Buenos Aires, Argentina.

0148-0227/09/2008JC004900

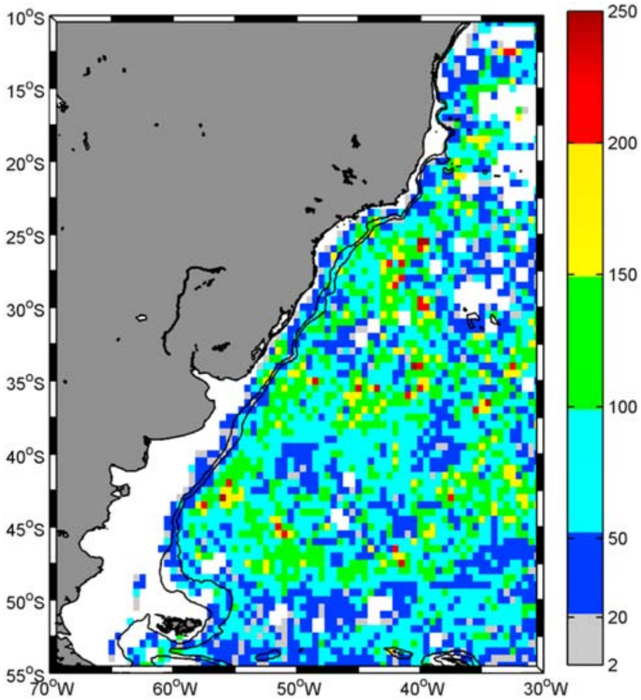

Figure 1. Number of independent drifters observations available within 0.5° × 0.5° bins. White bins mean either no data is available or the bin was visited by only one drifter with less than 20 observations (see text). The 200 and 1000 m isobaths are shown in black.

MC is a branch of the Antarctic Circumpolar Current and is thought to be controlled primarily by high-latitude dynamics [*Matano et al.*, 1993]. Near 38°S–40°S, the two western boundary currents converge to form the Brazil-Malvinas Confluence (BMC), one of the most energetic regions of the world ocean [e.g., *Legeckis and Gordon*, 1982; *Chelton et al.*, 1990; *Cirano et al.*, 2006]. The BMC is created by the head-on collision of the BC and MC. After colliding the currents veer offshore and form an intense, relatively narrow frontal system and an associated jet characterized by large variability. To date, details of the basic dynamical balances and eddy conversion processes in the BMC are poorly understood.

[7] With the recent increase in spatial and temporal coverage, surface drifters provide one of the best sources of information on the velocity field for estimating energetics in remote oceanic areas [*Niiler*, 2001]. Such estimates of energy exchange from ocean measurements may also provide a primary test for the performance of numerical models. Several studies have used this approach in the northern hemisphere [e.g., *Brügge*, 1995; *Baturin and Niiler*, 1997; *Lee et al.*, 2001]. *Fratantoni* [2001] used available surface drifter derived velocity data to investigate the energetics in the North Atlantic. The study describes the construction of a drifter climatology, which is based on the decadal mean quasi-Eulerian velocity and eddy kinetic energy fields on a 1° × 1° grid, and compared these results with contemporary satellite measurements. The maximum instantaneous velocity determined from a single drifter observation was 273 cm s^{-1} in the Gulf Stream southeast of Cape Cod and the highest eddy kinetic energy, 2790 cm^2 s^{-2}, was found in the Gulf Stream further downstream.

[8] Comparatively, in the South Atlantic, very few studies have been carried out to date. *Piola et al.* [1987] compiled a data set of 280 drifting buoys and prepared maps of mean surface velocity, kinetic energy and momentum flux on a 4° × 4° grid between 20°S and 68°S, providing an initial evaluation of those fields in the southern hemisphere. More recently, *Assireu et al.* [2003] used data from 15 drifters to provide detailed aspects of the surface circulation and kinetic energy along the BC between 24°S and 37°S.

[9] Eddy processes play two important roles in the mean kinetic energy balance: kinetic energy conversion and kinetic energy redistribution [e.g., *Nishida and White*, 1982]. The kinetic energy of the flow field in the ocean is dominated by mesoscale eddies with spatial scales of about 50–200 km at midlatitudes [*Morrow et al.*, 2004; *Lentini et al.*, 2006]. Given the energetic eddy field associated with the BC, MC and BMC and the general importance of these oceanic features to the South Atlantic, a number of observational and theoretical studies are needed to clarify the eddy mean flow interactions in that region.

[10] In the present study, we extend on the analysis of *Piola et al.* [1987] taking advantage of a much more robust data set available to date: 13 years of surface drifters data in the South Atlantic. Furthermore, the current database consists of a more uniform design of drifters, with improved water following properties and less sensitive to windage effects [*Niiler and Paduan*, 1995]. The current data set allows for a finer resolution grid which, for the first time, allows an adequate resolution for depicting the major surface circulation patterns and unveils several aspects of the eddy mean flow interactions in the area.

[11] The study area in the western South Atlantic spans between 10°S and 55°S and 70°W and 30°W, Figure 1, but our analysis focuses on the energetics of the BC. The remainder of this article is structured as follows: in the section 2 we describe the data set used and the statistical treatment applied to the analysis, the properties of the mean circulation and the kinetic energy distribution and barotropic conversion of kinetic energy are discussed in section 3. Summary and concluding remarks are given in section 4.

2. Data and Methods

[12] The surface drifters were developed under the Surface Velocity Program (SVP) of the Tropical Ocean Global Atmosphere (TOGA) experiment and the World Ocean Circulation Experiment (WOCE). The drifters were equipped with a holey-sock-type drogue centered at 15 m depth and were designed to minimize surface drag by both wind and waves [*Sybrandy and Niiler*, 1992]. Undrogued drifters were excluded from the analysis. The surface drifter data set used in this study spans a period of about 13 years, from January 1993 to December 2005. Also, we have included in the analysis some data available from 1990. For 1991 and 1992, the database has not valid records available for the analysis. The data was obtained from public archives of the Global Drifter Data Assembly Center at the National Oceanographic and Atmospheric Administration's Atlantic Oceanographic and Meteorological Laboratory (NOAA AOML, http://www.aoml.noaa.gov/phod/dac/gdp.html).

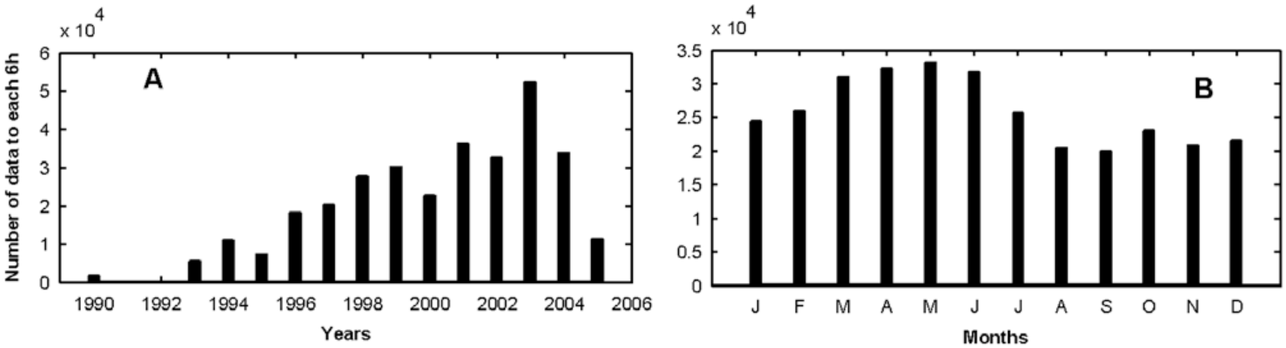

Figure 2. Number of 6 hourly velocity estimates ($\times 10^4$) per year (a) from 1990 to 2005 and (b) distributed by month.

[13] Gaps in the data, including those resulting from the operation of drifters on a one-third duty cycle (i.e., transmitter activated 1 day out of 3, or 8 out of 24 hours) were filled using a kriging technique developed by the AOML group [*Hansen and Herman*, 1989]. The final data generated by AOML, consists of 6 hourly interpolated position and surface temperature and velocity.

[14] Processing of the data at AOML, including acquisition of raw data from Argos satellite service and initial quality control is described in detail by *Hansen and Herman* [1989] and *Hansen and Poulin* [1996]. The amount of drifter data within the selected domain is 308,982 buoy days (number of drifters multiplied by number of days, with drifter positions available every 6 hours). The drifter sampling of our study domain increases considerably from about 5,000 buoy days/year in 1993 to about 40,000 buoy days/year after 2000 (Figure 2a).

[15] High-frequency fluctuations like inertial oscillations and tidal motions, which are out of the scope of this study, were removed using a 70 hours Butterworth low-pass filter applied to the velocity and temperature data [*Emery and Thomson*, 1998].

[16] All properties of the near surface circulation, which will be discussed in sections 3 and 4, were estimated by averaging the velocity data onto a geographical grid of fixed resolution. We used the classical "binning" method [e.g., *Owens*, 1991], i.e., grouping the velocity data in bins of selected size. The resulting values represent space-time averages over the grid elements and two different requirements should be fulfilled: each box should be as small as possible to reach a good spatial resolution and to obtain nearly homogeneous and stationary conditions as required by *Taylor*'s [1922] theory; and the number of data per box should be large enough to obtain statistically significant results.

[17] Our analysis showed that the grid resolution which resulted both in statistically reliable data and in finer resolution velocity fields was a grid with bins of 0.5° longitude × 0.5° latitude. The grid size was chosen to give a reasonable depiction of major ocean circulation features, particularly western boundary currents and the Brazil-Malvinas Confluence, while ensuring that most boxes contain sufficient data to form statistically reliable mean values. Measurements in a given box were judged to be independent if (1) they resulted from different drifters or (2) they resulted from the same drifter but that drifter remained in the box for more than one Lagrangian integral time scale (T). T is defined as the integral of the autocorrelation function from zero lag to the first zero crossing. A typical autocorrelation function from the Brazil Current region is depicted in Figure 3. This distribution is representative of the full domain. Since T ranges between 0.25 and 6 days over most of the domain, we choose a decorrelation scale of 5 days. This choice decreases the number of degrees of freedom and thus the errors calculated are maximum errors. Hence, in Figure 1, bins are marked white if no data is available or the particular bin contained data from only one drifter with less than twenty observations. After the application of the above criteria, our spatial resolution is higher than used in previous studies in the South Atlantic, which were based on a much smaller number of drifters [*Patterson*, 1985; *Piola et al.*, 1987; *Ishikawa et al.*, 1997]. Furthermore, the present grid has the order of the first Rossby radius of deformation at the domain's midlatitude. Data density in a given area is a function of both initial deployment density and of the regional circulation. Despite the substantial increase in the amount of data available in recent years, Figure 1 shows that the data coverage is rather heterogeneous, mostly as a result of the ocean circulation influence on the drifter distribution and to a lesser extent on the deployment pattern, which normally follow the busy merchant ship routes. Nevertheless, we consider the available data set to be robust enough to fulfill the objectives proposed in this study.

[18] Within each 0.5° × 0.5° box, the east ($\overline{u}$) and north ($\overline{v}$) components of the mean vector velocity were computed as follows. The drifter velocity data (selected as described above) were binned and the mean velocity calculated individually for each grid element and velocity components

$$\overline{u}_b = \frac{1}{N} \sum_{\substack{i=1 \\ i \text{ in box b}}}^{N} u_i \quad \text{and} \quad \overline{v}_b = \frac{1}{N} \sum_{\substack{i=1 \\ i \text{ in box b}}}^{N} v_i. \tag{1}$$

With i running over all drifter days within a given grid element (b) and where N is the total number of velocity observations within each grid element. The overbar denotes the bin average of the velocity components in the spatial bins. According to *Schäfer and Krauss* [1995], the mean velocity components are presented together the errors E of the mean value and root-mean-square (RMS) velocity which are dependent on $\sqrt{u'^2}/\sqrt{Nm}$ where Nm is the number of independent samples which is related to the Lagrangian integral time scale T by $Nm = N/2T$ (taken here to be 5 days throughout the domain), N being the number of

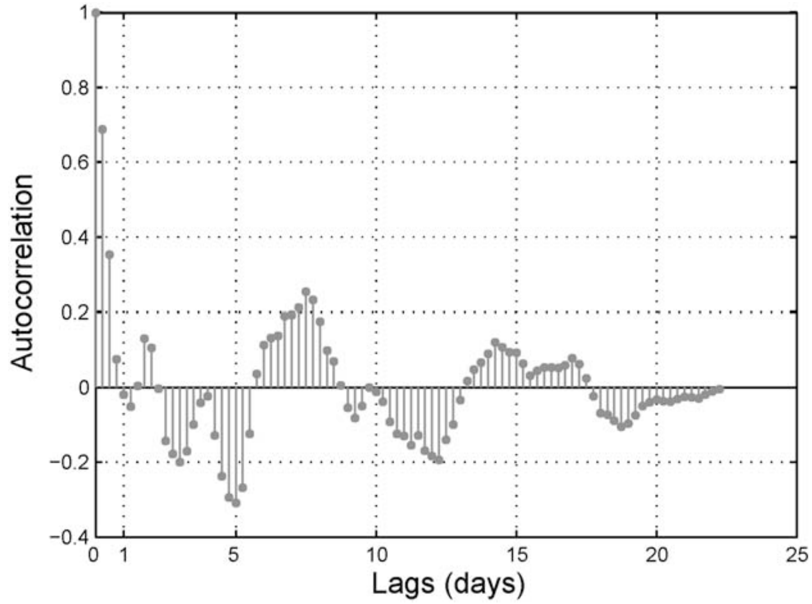

Figure 3. Autocorrelation function for $\overline{v}$ estimated on transect VI on the grid element located nearest to the Brazil Current core.

velocity observations within each grid element. For a 95% confidence interval according to Student's test we have

$$\overline{u} \pm E = \overline{u} \pm \frac{2\sqrt{\overline{u'^2}}}{\sqrt{Nm}} \quad \text{and} \quad \overline{v} \pm E = \overline{v} \pm \frac{2\sqrt{\overline{v'^2}}}{\sqrt{Nm}} \tag{2}$$

and the RMS error velocity

$$\sqrt{\overline{u'^2}} \pm E = \sqrt{\overline{u'^2}} \pm \frac{2\sqrt{\overline{u'^2}}}{\sqrt{2Nm}} \quad \text{and} \quad \sqrt{\overline{v'^2}} \pm E = \sqrt{\overline{v'^2}} \pm \frac{2\sqrt{\overline{v'^2}}}{\sqrt{2Nm}}. \tag{3}$$

The binning process resulted in time series of velocity components for each grid element. The next step was to remove the mean from these series in order to separate the mean and the eddy velocities, so that each velocity component could be divided into its temporal mean $\overline{u}$ and its instantaneous deviation u'

$$u = \overline{u} + u', v = \overline{v} + v'. \tag{4}$$

The mean product of the perturbation velocities were derived for each grid element "b" by

$$\overline{u'u'}_b = \frac{1}{N}\sum_{\substack{i=1\\ i \text{ in box b}}}^{N} u'_i u'_i \quad \text{and} \quad \overline{v'v'}_b = \frac{1}{N}\sum_{\substack{i=1\\ i \text{ in box b}}}^{N} v'_i v'_i. \tag{5}$$

Energy calculations are usually made with currents rotated relative to the local topography or into a coordinate system which maximizes variance in the principal direction. We tested the effect of decomposing the currents in alongshore and cross-shore directions but results were essentially unchanged. While the international recommendation is to use the International System units (SI), the CGS units were used here to facilitate direct comparison with previously published results.

[19] Using this data set, we estimate the distribution of kinetic energy per unit mass for the mean and eddy fields as follows. The total kinetic energy was divided into two parts: the kinetic energy of the mean flow per unit mass (MKE) and the eddy kinetic energy per unit mass (EKE). MKE generally represents the energy of the large-scale mean circulation (record length) and is here directly associated with the mean drift velocities. EKE results are obtained from the fluctuating part of the absolute velocity. According to *Schäfer and Krauss* [1995], after removing high-frequency fluctuations the turbulent velocity components in the ocean, u' and v', are mainly due to eddies and meanders. In our case, the high-frequency oscillations were removed by the temporal filtering during the initial processing steps and thus it is likely that the turbulent velocity components contain essentially information from the mesoscale field.

[20] EKE and MKE distributions are calculated assuming that the mean velocity was centered geographically at the center of each grid box. Since the time averages are computed over many years (13 years), the eddy statistics presented include the contributions from all eddy scales. MKE and EKE were calculated as follows:

$$\text{MKE}_b = \frac{1}{2}\left(\overline{u}_b^2 + \overline{v}_b^2\right) \quad \text{and} \quad \text{EKE}_b = \frac{1}{2}\left(\overline{u'u'}_b + \overline{v'v'}_b\right). \tag{6}$$

We also estimated the barotropic conversion of energy from the mean flow to the eddy field. The barotropic conversion term is calculated as follows:

$$\text{BT} = -\left[\overline{u'u'}\frac{\partial\overline{u}}{\partial x} + u'v'\left(\frac{\partial\overline{u}}{\partial y} + \frac{\partial\overline{v}}{\partial x}\right) + \overline{v'v'}\frac{\partial\overline{v}}{\partial y} + \overline{w'v'}\frac{\partial\overline{v}}{\partial z} + \overline{w'u'}\frac{\partial\overline{u}}{\partial z}\right]. \tag{7}$$

Where, $\overline{u'u'}, \overline{v'v'}, \overline{u'v'}, \overline{w'v'}$ and $\overline{w'v'}$ are the Reynolds stress tensors per unit mass (equation (7)) and $\frac{\partial\overline{u}}{\partial x}, \frac{\partial\overline{u}}{\partial y}, \frac{\partial\overline{v}}{\partial x}, \frac{\partial\overline{v}}{\partial y}$ are the horizontal gradients of the mean velocity components

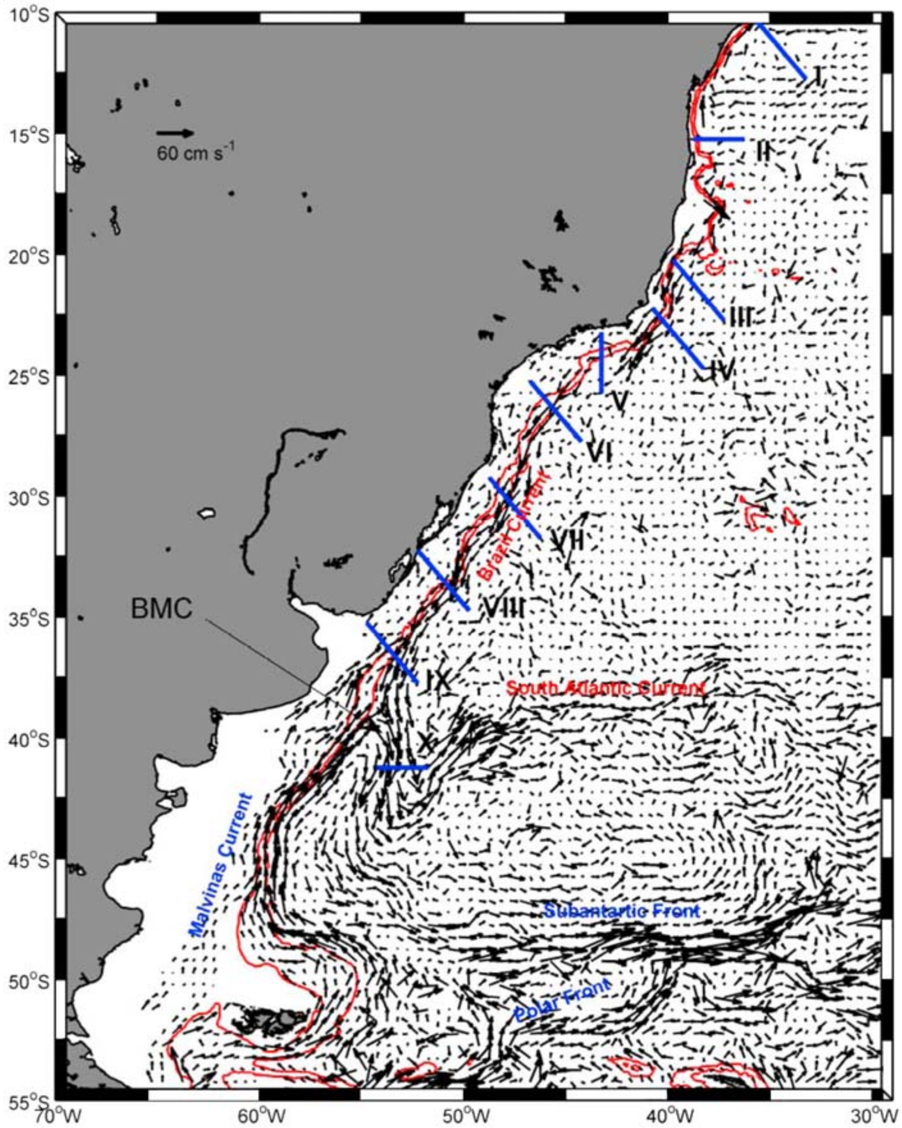

Figure 4. Mean surface velocity field in the western South Atlantic derived from 0.5° × 0.5° grid. Vector lengths are directly proportional to the velocity magnitude (see scale). Also shown are the 200 and 1000 m isobaths. Tansects I–X are labeled.

barotropic conversion (BT) is the time mean calculated for each grid element.

[21] BT includes a part proportional to the horizontal current shear (barotropic conversion) and a part proportional to the vertical shear (Kelvin-Helmholtz conversion). Here, we neglect the Kelvin-Helmholtz conversion terms $(\overline{w'v'}\frac{\partial\overline{v}}{\partial z}+\overline{w'u'}\frac{\partial\overline{u}}{\partial z})$ because this conversion contributes mainly to daily and shorter fluctuations, which were previously removed during the temporal filtering process [*Grodsky et al.*, 2005]. BT represents the rate of generation of EKE by the interaction of the Reynolds stresses with the mean shear components, which can be interpreted in terms of the direction of eddy momentum flux relative to the mean momentum gradient [e.g., *Dewar and Bane*, 1989; *Wilkin and Morrow*, 1994]. Positive values of BT indicate that the eddy fluxes are down gradient and therefore energy transfer from the mean flow to the eddy field [e.g., *Bryden*, 1982; *Rossby*, 1987; *Hall*, 1991; *Cronin and Watts*, 1996; *Azevedo et al.*, 2008]. Thus, in summary BT > 0 implies MKE → EKE. Conversely, negative values of BT indicate conversion from EKE to MKE, which mean that eddies are decaying accelerating the mean flow.

3. Results and Discussion

3.1. Mean Surface Circulation

[22] The drifter derived mean surface velocity field unveils circulation details associated with the western branch of the South Atlantic gyre (Figure 4). The major currents better defined by the Lagrangian data are the southward flowing Brazil Current, along the western boundary of the subtropical gyre, the northward flowing Malvinas Current, along the western edge of the Argentine Basin and their encounter near 38°S, creating the Brazil-Malvinas Confluence. In the BMC, the mean current appears as a

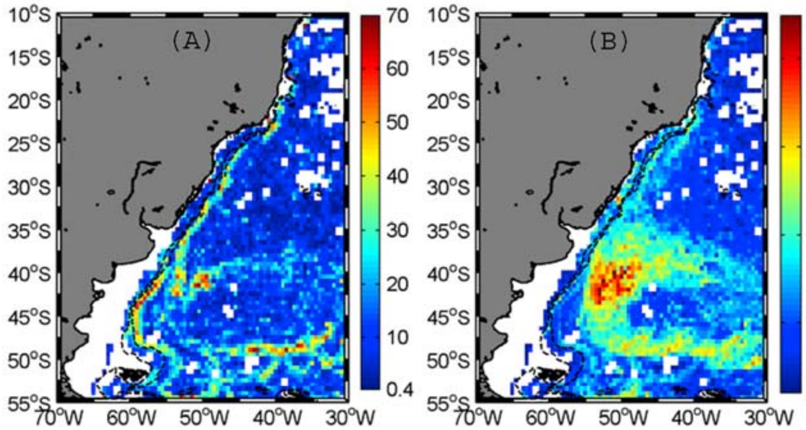

Figure 5. (a) Surface mean speed ($V = \sqrt{\overline{u}^2 + \overline{v}^2}$) distribution in cm s^{-1} and (b) standard deviation of the mean speed in cm s^{-1}. Also shown are the 200 and 1000 m isobaths.

broad poleward flow centered around 53°W, penetrating south to 42°S where it describes a sharp anticyclonic turn and a subsequent northeastward flow to 40°S–50°W. At this point the surface flow decreases substantially and a broad meandering eastward flow marks the origin of the South Atlantic Current (SAC) [*Stramma and Peterson*, 1990]. The data also clearly depict the relatively strong flows associated with the Antarctic Circumpolar Current. The Subantarctic Front (SAF) is observed along the southern flank of the Argentine Basin (Figure 4, ~49°S). Also the zonal flow associated with the Polar Front near 52°S veers northward at around 42°W and merges with the SAF at 49°S–40°W [see also *Orsi et al.*, 1995].

[23] The high resolution of our grid and the relatively large number of available velocity data lead to realistic values of mean surface velocity in the western South Atlantic. The highest mean velocities (~60 cm s^{-1}) are found near the western boundary in the MC and BMC domains and in the BC (~50 cm s^{-1}, Figure 5a). Mean surface velocities are also observed along the Subantarctic Front (~49°S). East of the BMC the mean velocity gradually decrease (<30 cm s^{-1}) along the path of the SAC away from the western boundary. In the region located southeast of the BMC, known as the Zapiola Drift or Zapiola Anticyclone [*Saunders and King*, 1995; *Saraceno et al.*, 2005], mean velocities are of the order of 10 cm s^{-1}. Elsewhere, in the deep oceanic basins and away from sharp bottom topography, mean surface velocities are generally low (<10 cm s^{-1}).

3.2. Surface Circulation Variability

[24] The standard deviation of the surface velocity field is frequently used as a *proxy* of the surface circulation variability (Figure 5b). The region with highest variability is concentrated near the BMC, where the standard deviations (40 cm s^{-1}) are comparable to the mean. Using a variety of methods (e.g., sea level, velocity and SST variability) several studies have shown that the BMC is one of the most energetic regions of the world ocean [*Cheney et al.*, 1983; *Chelton et al.*, 1990]. The large variability is due the frequent shedding of large eddies and rings [e.g., *Tomczak and Godfrey*, 1994; *Fu et al.*, 2001]. The variability tends to decrease as the BMC meanders offshore toward the SAC. High standard deviations (~30 cm s^{-1}) are also observed along the Subantarctic front (SAF) (Figures 5a and 5b), bordering the Falkland Escarpment further south. This is in

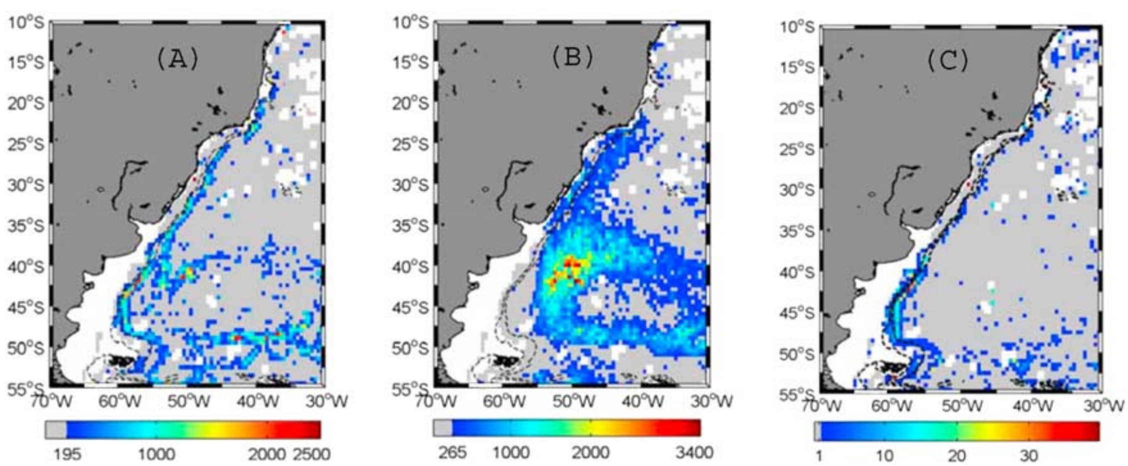

Figure 6. (a) Distribution of kinetic energy of the mean flow per unit mass in cm^2 s^{-2}, (b) distribution of eddy kinetic energy per unit mass in cm^2 s^{-2}, and (c) ratio of mean kinetic energy to eddy kinetic energy. Also shown are the 200 and 1000 m isobaths.

agreement with the observations of *Hofmann* [1985], who analyzed near-surface drifting buoys from the First GARP Global Experiment (FGGE) and found averaged speeds of about 40 cm s^{-1} in the SAF.

[25] High standard deviations have also been observed along the path of the WBCs [*Hogg and Johns*, 1995]. In the BC, the variability in the southern region is more heterogeneous, and the highest values (30 cm s^{-1}) are found after separation from the shelf break (Figure 5b). High variability is also observed in the South Brazil Bight shelf break and slope between 23°S–30°S and 50°W–40°W, where BC eddies have been frequently reported [e.g., *Campos et al.*, 2000]. Furthermore, within the Brazil Current domain the standard deviation of the surface velocity can also be relatively high when compared with the mean velocity in some areas (e.g., near Cabo Frio, ~23°S), which results from the important role that the eddy field plays in the BC dynamics along its path.

3.3. Kinetic Energy Fields

[26] The Mean Kinetic Energy and Eddy Kinetic Energy fields are shown in Figures 6a and 6b, respectively. The highest MKE values are found along the path of the WBCs, particularly in the MC north of 45°S, where values approaching 2500 cm^2 s^{-2} were computed. The SAF and the offshore branch of the BMC retroflection meander also show locally enhanced levels of MKE (~1000 cm^2 s^{-2}). On the basis of a resolution grid of 2° × 2°, *Ishikawa et al.* [1997] estimated MKE values of 1000 cm^2 s^{-2} at the MC and BC, but their estimates could still be affected by the low drifter density in the area.

[27] The EKE field is a combined measure of the current spatial and temporal variability within each grid element and is normally associated with mesoscale activity. The highest EKE was found in the vicinity of the BMC, where values approach 3000 cm^2 s^{-2} (Figure 6b). High EKE in the BMC has been attributed to the frequent observation of mesoscale eddies and meanders. The high values found in the BMC are in agreement with previous studies in the area which estimated the EKE field from different data sources [*Patterson*, 1985; *Piola et al.*, 1987; *Ishikawa et al.*, 1997]. Despite the qualitative agreement between these EKE distributions, the estimates in the present study are based on a larger number of drifters and on a finer resolution binning and hence are significantly higher. Thus, the improved observations allow a more accurate assessment of the mesoscale contribution to the total energy budget in the southwestern Atlantic.

[28] Locally enhanced EKE observed along the SAF may be associated with the interaction of the ACC with the Falkland Escarpment, where the SAF and the Polar Front converge [*Wilkin and Morrow*, 1994]. In addition to the major topographic features that may increase the flow variability, several additional ridge structures may also be sources of increased eddy kinetic energy [*Gille*, 1997]. Those interactions are likely to favor the triggering and growth of mean flow instabilities and enhance eddy activity. When compared to the BC, the MC displays lower values of EKE (<265 cm^2 s^{-2}) indicating that the eddy activity is lower in the latter. Indeed, when comparing the EKE with the MKE (Figure 6c, discussed below), the MC displays a clear dominance of the mean flow over the eddy variability. One factor that contributes to the low EKE values found in the MC is its barotropic nature, which makes it more effectively steered by the continental slope [*Vivier and Provost*, 1999]. The low EKE region (<265 cm^2 s^{-2}) surrounded by the BMC and the SAF maxima characterizes the Zapiola Anticyclone. The latter also stands out as a region of low sea surface height variability (RMS < 15 cm) on the basis of satellite altimeter [*Goni and Wainer*, 2001] and presents distinct color and sea surface temperature patterns [*Saraceno et al.*, 2005].

[29] The MKE/EKE ratio presents considerable spatial variability (Figure 6c). Over most areas of the western South Atlantic, the EKE is higher than the MKE. Only within the principal axis of the Brazil and Malvinas currents MKE > EKE (Figure 6c). The dominance of EKE over MKE away from the western boundary has been reported by several studies and reflects the eddy nature of the upper ocean [e.g., *Wyrtki et al.*, 1976; *Piola et al.*, 1987; *Oort et al.*, 1989]. However, inspecting Figure 6c in the southwestern Atlantic boundary currents it is evident that MKE becomes more important, especially in the MC as discussed above.

[30] In contrast, along the path of the WBC the strong and steady mean flows favor the dominance of MKE over EKE. Sections 3.4, 3.5, and 3.6 focus on the energy fields in the western boundary systems. Special attention is given to the BC and associated features.

3.4. Brazil Current

[31] In contrast with all previous studies [e.g., *Patterson*, 1985; *Piola et al.*, 1987] our analysis reveals that over most of the BC the MKE is higher than the EKE. North of 35°S along the BC path, the MKE values range from 95 to 1314 cm^2 s^{-2}, while the EKE levels are generally lower than 500 cm^2 s^{-2}, see Table 1. Using data from surface drifters drogued at 5 and 30 m depth on a 5° × 5° grid, *Patterson* [1985] estimated MKE values lower than 50 cm^2 s^{-2} in the core of the BC. As the cross-current scale of the BC is ~100–150 km, low MKE estimates are probably associated with the low spatial resolution in that study. The lack of spatial resolution in a relatively narrow flow like the BC should also have affected the results obtained by *Piola et al.* [1987], who found MKE of 200 cm^2 s^{-2} using a 4° × 4° grid in the area. Further downstream, the typical MKE in the BMC is 1116 cm^2 s^{-2}, with peaks of 2500 cm^2 s^{-2}. These estimates are much higher than the 50 cm^2 s^{-2} estimated by *Wyrtki et al.* [1976] and the 200 cm^2 s^{-2} estimated by *Patterson* [1985] and *Piola et al.* [1987].

[32] Along the path of the BC, the associated EKE field shows a large range of values varying from 131 to 838 cm^2 s^{-2} (Table 1). *Wyrtki et al.* [1976] reported EKE over the BC between 600 and 800 cm^2 s^{-2}, again probably due to the low spatial resolution (5° × 5°) of their analysis. As suggested by *Richardson* [1983], these relatively high EKE estimates may be associated with the original ship drift data from which the velocity was derived. *Wyrtki et al.* [1976] EKE distribution does not resolve the mesoscale eddies, because ship drift data are averaged over a 1 day navigation period, which, on average corresponds to about 400 km. Thus, ship drift data inherently underestimate the variance in the velocity field because of mesoscale phenomena and the associated kinetic energy. More recently using a few surface drifters, *Assireu et al.* [2003] found EKE values in the BC ranging from 340 to

Table 1. Mean Speed ±*E*, Standard Deviation ±*E*, Mean Alongshore Velocity ±*E*, Mean Alongshore Velocity Standard Deviation ±*E*, Mean Kinetic Energy, Eddy Kinetic Energy, Barotropic Conversion, and the Estimated Distance of the BC Principal Axis to the 200 m Isobath[a]

Transect	Latitude (°S)	Longitude (°W)	Speed (cm s^{-1})	SD (cm s^{-1})	v (cm s^{-1})	SD v (cm s^{-1})	MKE (cm^2 s^2)	EKE (cm^2 s^2)	BT (cm^2 s^{-3})	Distance to the 200 m Isobath (km)
I	10.25	35.75	21.32 ± 20.4[b]	13.74 ± 14.4	21.21 ± 18.2[b]	12.23 ± 12.9	227.43	284.21	-4.10^{-3}	–
II	15.25	37.25	13.83 ± 8.1[b]	10.67 ± 5.7[b]	−8.0 ± 14.5	19.10 ± 10.2[b]	95.60	262.0	7.10^{-4}	–
III	20.25	39.75	29.45 ± 14.9[b]	13.74 ± 10.5[b]	−27.83 ± 16.7[b]	15.45 ± 11.8[b]	433.78	131.62	1.10^{-4}	9
IV	22.75	40.75	50.61 ± 19.2[b]	19.75 ± 13.6[b]	−39.8 ± 23.1[b]	24.47 ± 16.8[b]	1280.0	473.00	4.10^{-3}	47
V	24.25	43.25	17.20 ± 13.7[b]	15.33 ± 9.7[b]	−2.87 ± 15.7	17.62 ± 11.1[b]	147.87	359.73	-1.10^{-3}	40
VI	26.25	47.75	39.42 ± 17.2[b]	25.85 ± 12.1[b]	−27.17 ± 17.9[b]	26.95 ± 12.7[b]	776.0	612.93	3.10^{-3}	43
VII	30.25	47.75	51.28 ± 14.6[b]	16.0 ± 10.3[b]	−47.07 ± 18.2[b]	19.9 ± 12.8[b]	1314.0	282.09	-5.10^{-4}	67
VIII	33.75	50.75	43.24 ± 14.2[b]	17.87 ± 10.0[b]	−34.61 ± 14.7[b]	18.52 ± 10.4[b]	934.91	265.00	9.10^{-4}	26
IX	36.75	53.25	32.33 ± 17.9[b]	24.12 ± 12.7[b]	−32.15 ± 25.1[b]	33.67 ± 17.7[b]	522.71	838.62	7.10^{-3}	68
X	41.25	53.75	47.25 ± 22.9[b]	36.40 ± 16.2[b]	−46.92 ± 27.2[b]	43.26 ± 19.2[b]	1116.0	1400.0	-1.10^{-3}	377

[a]Here SD is standard deviation, v is mean alongshore velocity, SD v is mean alongshore velocity standard deviation, MKE is mean kinetic energy, EKE is eddy kinetic energy, and BT is barotropic conversion.
[b]The results that are statistically significant.

495 cm^2 s^{-2} for the 1993–1994 period. The absence of seasonal EKE variations seems to be a common feature of subtropical WBCs, as suggested by *Ishikawa et al.* [1997]. The study domain does not exhibit particularly distinct seasonal variations on the EKE fields (see Figure 2b).

[33] Further detailed results in the BC fields are presented in Table 1 and Figures 4–7. Table 1 shows the mean velocity values, the associated variability and the kinetic energy levels compiled from transects across the BC principal axis at several latitudes along the current's path. The transects are shown in Figure 4. The northernmost transect (I), centered at 10.25°S–35.75°W, presents no evidence of southward flow as the surface current is northward along the entire transect (Figure 7, transect I). This observation agrees with the geostrophic calculations of *Stramma and England* [1999], which showed no evidence of poleward flow at 100 m at similar latitudes. At the surface, the southward flowing Brazil Current (BC) is apparent south of the bifurcation of the South Equatorial Current and is evident in the transect II (15.25°S–37.25°W) with mean meridional (alongshore) velocities of 8 ± 14.5 cm s^{-1} southward (Table 1). At this location the variability is 19 ± 10.2 cm s^{-1}, which is larger than the mean, suggesting that the current may also revert and flow northward from time to time. This observation is probably due to the proximity to the South Equatorial Current bifurcation (i.e., origin of the Brazil Current and the North Brazil Current), which in the mean is apparent near 15°S (Figure 4).

[34] At 20.25°S–39.75°W, the BC flow is better defined and consistent between the 200 and 1000 m isobaths (Figure 4, transect III) in agreement with previous studies in the area [*Peterson and Stramma*, 1991]. The mean southward (alongshore) flow reaches 27 ± 16.7 cm s^{-1} associated with high levels of variability (standard deviation v = 15.4 ± 11.8 cm s^{-1}; see Table 1 (transect III)). The increase of the BC surface velocity continues southward over the continental slope, between the 200 to 1000 m isobaths (Figure 4, transect IV) reaching a peak value near 22.75°S (39 ± 23.1 cm s^{-1} standard deviation v = 24.4 ± 16.8 cm s^{-1}).

[35] Further south, as the BC enters the South Brazil Bight (SBB) the coastline and slope turn sharply westward becoming approximately zonal, leading to the formation of a quasi-stationary meander off Cabo Frio (~23°S) as the current overshoots away from the continental slope [*Calado et al.*, 2006]. The development of instabilities result in higher EKE levels (359 cm^2 s^{-2}) in transect V, with variability levels (17.6 ± 11.1 cm s^{-1}) becoming larger than the mean alongshore current (−2.82 ± 15.7 cm s^{-1}, Table 1). Cyclonic eddies of about 40 km diameter frequently observed at this location have been associated with the combined effects of baroclinic instability of the BC and the local increase of the bottom slope at the shelf break near 23°S [*Assireu et al.*, 2003]. This may explain why the surface MKE/EKE ratio decreases at this location. Along its poleward path, at the surface the BC picks up speed again, reaching its maximum near 30°S (47.0 ± 18.2 cm s^{-1} standard deviation v = 19.9 ± 12.8 cm s^{-1}, transect VII). Close to the same location and on the basis of current meter data, *Müller et al.* [1998] found even higher variability (mean equals 30 cm s^{-1}, standard deviation equals 22 cm s^{-1}) at the BC subsurface core (120 m). Elsewhere, in the deeper basin away from the continental boundary the surface velocity variability levels are generally low (≤15 cm s^{-1}).

[36] The BC separates from the coast near transect IX (36.75°S–53.25°W) and becomes a free oceanic jet at ~38°S. Around that position the BC surface mean speed is ~32 ± 17.9 cm s^{-1} with associated variability of 24 ± 12.7 cm s^{-1}. This is in contrast with previous studies and other southern hemisphere western boundary currents, where EKE > MKE is suggested [*Patterson*, 1985; *Piola et al.*, 1987; *Ishikawa et al.*, 1997]. Indeed this result is most likely associated with the enhanced spatial resolution of our velocity binning, and suggests that new estimates for other western boundary currents with improved resolution might also lead to higher MKE values.

[37] The northward return of the Brazil Current is observed at the eastern end of the southernmost transect (transect X, see Figure 7). At that location, the estimated EKE = 1739 cm^2 s^{-2} while MKE = 746 cm^2 s^{-2}, confirming previous findings which suggest the strong role of the eddy field in this region. Although very high in oceanic terms, the maximum EKE value for the BC is still about half of highest EKE (1000–1500 cm^2 s^{-2}) estimated in the Gulf Stream near 35°N–74°W on the basis of similar approach and database [*Fratantoni*, 2001].

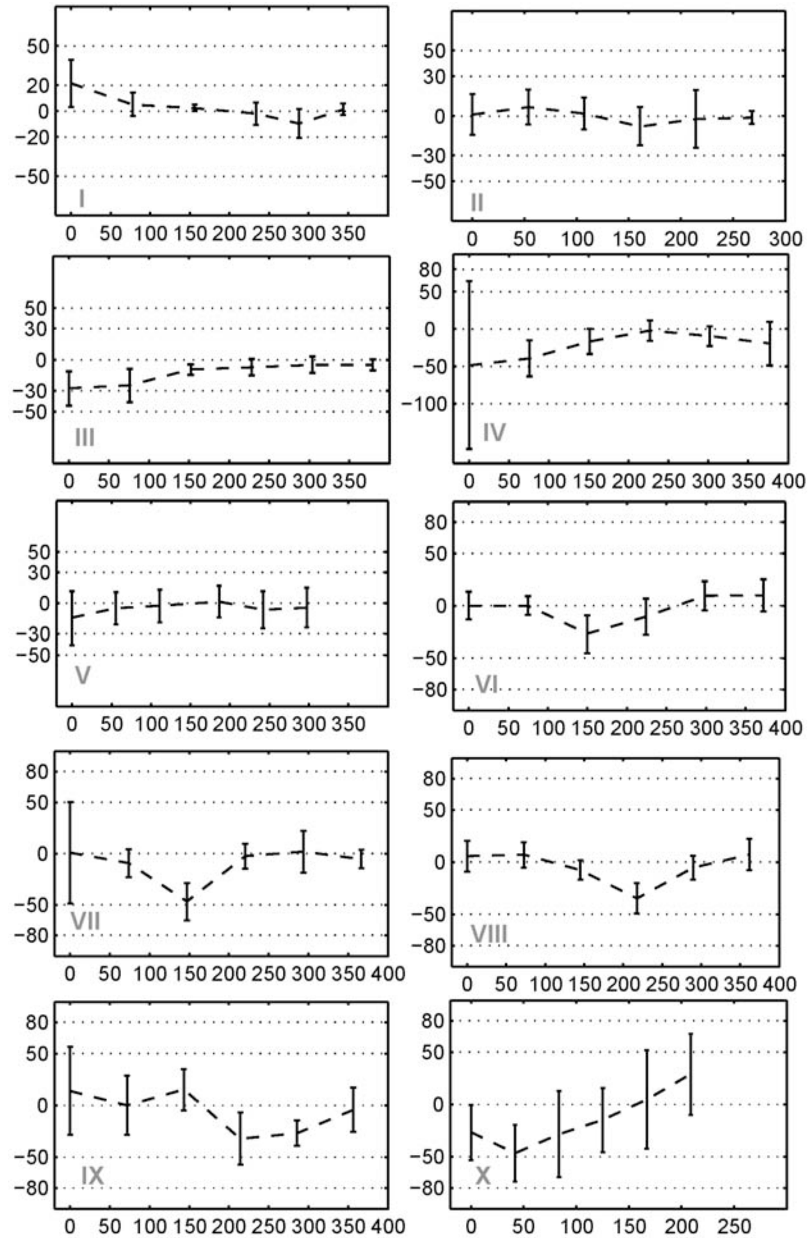

Figure 7. Mean cross-shore distribution of alongshore velocity with errors bars on selected transects in cm s^{-1}. Tansects I–X are shown.

3.5. Malvinas Current

[38] The surface expression of the MC core is located between the 200 m and 1000 m isobaths (Figure 4). Near 39°S, the MC separates from the continental margin, describes a sharp cyclonic loop, and veers southward as part of the Brazil-Malvinas Confluence. The mean velocity of the southward flow is about 30 cm s^{-1} (Figure 4). The surface MKE in the MC is higher than 1000 cm^2 s^{-2} and at some locations it is higher than 2000 cm^2 s^{-2} (Figure 6a). *Wyrtki et al.* [1976] with a 5° binning found that the MKE < 50 cm^2 s^{-2} in the MC, while *Piola et al.* [1987] with and improved grid and data set estimated an MKE of 500 cm^2 s^{-2}.

[39] In the MC the EKE does not exceed 265 cm^2 s^{-2} (see Figure 6b), this value is lower than the previous estimates by *Wyrtki et al.* [1976], *Patterson* [1985], and *Piola et al.* [1987] of 600, 200, and 300 cm^2 s^{-2}, respectively. These estimates appear to be coherent with the adopted spatial resolution and the substantially lower number of observations on which these estimates were based.

3.6. Brazil-Malvinas Confluence

[40] The drifter derived mean surface velocities at the Confluence are around 30 cm s^{-1} and peaks of around 60 cm s^{-1} are observed (see Figure 5a). The BMC is surrounded by the Subantarctic Front, in the southern border and by the Subtropical Front in the northern border. At the BMC core the standard deviation of the surface velocity is 30 to 45 cm s^{-1} (Figure 5b). The latter value is very close to the observed mean in the region (Figure 5a), thus reflecting the high mesoscale variability in the area [e.g., *Piola et al.*,

1987]. Thus, the EKE field is also associated with large values raging between 1500 and 3500 cm^2 s^{-2}, even when compared to the Gulf Stream, which range from 1500 to 2800 cm^2 s^{-2} [*Fratantoni*, 2001]. Analysis of the seasonal distributions of EKE and MKE reveal no significant seasonal variability (see Figure 2b).

[41] Furthermore, our EKE estimates in the BMC show higher values than previous estimates based on coarser resolution grids and substantially fewer number of velocity estimates. For example, using ship drift data *Wyrtki et al.* [1976] found values of around 1000 cm^2 s^{-2}, while *Patterson* [1985] and *Piola et al.* [1987] using surface drifter data, estimated 1200 and 2000 cm^2 s^{-2}, respectively. All previous studies found relatively high EKE in the BMC, however, because of the limited spatial resolution and poor data coverage, they consistently underestimated the EKE in this region. Our results, based on a substantial increase in the number of drifters available after 2000, allowed an improved resolution and hence more robust estimates of EKE, MKE and associated fields.

3.7. Barotropic Conversion of Kinetic Energy (BT)

[42] The conversion of MKE to EKE is given by the BT term (equation (7)) and can be used as an indicator for barotropic instability [e.g., *Kundu and Cohen*, 1990]. Wherever this term is positive, MKE is being converted to EKE through the work of the Reynolds stresses on the mean shear. The Baroclinic Instability (BI) indicator [e.g., *Cushman-Roisin*, 1994; *Cronin and Watts*, 1996; *Biastoch and Krauss*, 1999] cannot be calculated from the current observations since estimates of time fluctuations of potential density field (ρ') are not available at the required space and time scales. Moreover, baroclinic instabilities are also expected to develop along the Brazil Current and can be evaluated, for example, with the aid of numerical experiments. *Silveira et al.* [2008] have studied the meandering of the BC at 22.7°S close to the 1250 m isobath using ten current meter moorings. The data depicted a strong frontal meandering event that lead to a current inversion where normally south-southwestward velocities associated to the BC are observed. The magnitude of our BT estimates along the path BC is similar to the BT term of the Gulf Stream calculated by *Cronin and Watts* [1996]. However, *Silveira et al.* [2008] concluded that the BC system is baroclinically unstable. Yet, we have no way to estimate the baroclinic conversion rate on the basis of the drifter data. Barotropic instabilities feed on the horizontal shear of the current, while baroclinic instabilities are dependent on the vertical shear. Hence, both types of instability can coexist [e.g., *Cushman-Roisin*, 1994].

[43] Focusing on the Brazil Current region (see Table 1), an area of significant MKE to EKE conversion occurs near transect IV, VI, VIII and IX, where the alongshore velocity of the BC is large, thus leading to largest horizontal shears and therefore increasing the potential to develop barotropic instabilities. Most of the transects in Table 1 present positive BT indicating conversion of MKE into EKE along the entire BC path. That is a relevant result as those instabilities have been linked to the formation and development of large rings at the separation latitudes of other southern hemisphere western boundary currents like the Agulhas [*Biastoch and Krauss*, 1999; *de Ruijter et al.*, 1999; *van Leeuwen et al.*, 2000] and the East Australian Current [*Bowen et al.*, 2005; *Mata et al.*, 2006].

[44] Transect V (near Cabo Frio, where the South American coastline sharply changes orientation) presents negative values, indicating conversion of EKE to MKE. Thus, at that location, mean kinetic energy increases at the expense of eddy kinetic energy and ultimately the mean flow is being accelerated by eddy decay. Eddy to mean kinetic energy conversion has been previously observed in other southern hemisphere currents. *Wilkin and Morrow* [1994] estimated BT in the Agulhas Current and found an area of significant EKE to MKE conversion west of the Agulhas Plateau, near 20°E–40°S, where the Agulhas eddies decay, feeding energy back to the mean flow. Similarly, *Mata et al.* [2006] estimated the BT field for the Tasman Sea using both altimetry and the outputs of a global ocean model. They found that the BT associated with the path of the EAC increases as the current approaches its separation latitude. Table 1 suggests a scenario with the BT term varying between O(10^{-4}) to O(10^{-3}), when the Brazil Current flows from transect III to transect X situated at the southern edge of its retroflection.

[45] Summarizing, along the core of Brazil Current we found potential for the development of barotropic instability (positive BT), i.e., eddies grow at the expense of the mean flow. Conversely, at other locations (transect V, VII, and approaching transect X), the small and/or negative values of BT suggest that eddies decay and feed energy into the mean flow through kinetic energy conversion.

4. Summary and Conclusions

[46] The objective of this study is to describe the mean near surface circulation and its energetics in the Southwestern Atlantic with emphasis on the Brazil Current and the Brazil-Malvinas Confluence. Accurate knowledge of these statistical properties is instrumental for understanding the near surface ocean dynamics and thus its variability. These results are particularly useful for assessing the performance of eddy-resolving ocean models.

[47] The velocity and energy statistics were estimated by averaging the available surface drifter velocities, spanning approximately 13 years, onto a 0.5° × 0.5° grid. The relatively large number of data allows us to make a finer scale map than was possible in previous studies and to better asses the role of the eddies in the general circulation. Since the distribution of the mean and the eddy kinetic energy is significantly affected by spatial (horizontal) resolution of the data set, our finer scale maps provide a substantially more realistic description of the surface circulation in the Southwestern Atlantic Ocean and its variability.

[48] We divided the kinetic energy estimates into its mean and eddy components. The highest alongshore velocity associated with the BC is 47 cm s^{-1} with RMS of 20 cm s^{-1} near 30.25°S–47.75°W. At that location, the MKE associated to the BC flow reaches 1314 cm^2 s^{-2} while EKE is 282 cm^2 s^{-2}. Our maps reveal that the MKE is larger than 1000 cm^2 s^{-2} in the core of western boundary currents of the South Atlantic, their extensions and in the Brazil-Malvinas Confluence. Conversely, EKE at the BMC is larger than 1500 cm^2 s^{-2}. Secondary EKE maxima are observed along the Subantarctic Front (~1500 cm^2 s^{-2}),

ultimately most of the kinetic energy of the surface circulation is in the eddy field. As described before, the EKE distribution over the BMC is comparable to the most energetic regions in the global ocean. Moreover, the similar values of MKE and EKE found in the BMC suggest strong interactions between the mean flow and the eddies which was confirmed by the analysis of *Oliveira* [2008] using a combination of drifter data and the outputs of a global ocean model.

[49] We have also provided the first available estimates of the barotropic conversion term for the Brazil Current path on the basis of surface drifter data. The BT estimates indicated conversion of mean kinetic energy to eddy kinetic energy, along most of the Brazil Current path, resulting from the development of barotropic instabilities. The one exception is at transect V (near 23°S Cabo Frio) and VII, where eddy to mean energy conversion is found. The increase of BT toward the southernmost extensions of the BC (transect IX and X) suggests that barotropic instability plays an important role in the formation of the BMC eddies, as observed in the other WBC of the southern hemisphere subtropical gyres (the Agulhas and the EAC). The estimate of the baroclinic conversion term and the relative importance between baroclinic and barotropic energy conversion mechanisms in this energetic region should be further investigated, for instance, with the aid of numerical models and in situ observations.

[50] **Acknowledgments.** This research was funded by grants 550370/2002–1 (GOAL) and 520189/2006–0 (SOS-CLIMATE) of the Brazilian Research Council/Brazilian Antarctic Program (CNPq/PROANTAR) and it was carried out with the aid of a grant from the Inter-American Institute for Global Change Research (IAI) CRN 2076, which is supported by the U.S. National Science Foundation (grant GEO-0452325). We also thank the support given by the Brazilian Ministry of the Environment (MMA) to GOAL activities. L.R.O. and M.M.M. were supported by a CAPES/FURG doctoral fellowship (BEX 382217/2007–1) and CNPq research grant (Pq 301623/2006–6), respectively. Additional funding was provided by PICT04-25533 from Agencia Nacional de Promocion Cientifica y Tecnologica, Argentina. The authors wish to thank AOML/NOAA for providing the drifter data.

References

Assireu, A. T., M. R. Stevenson, and J. L. Stech (2003), Surface circulation and kinetic energy in the SW Atlantic obtained by drifters, *Cont. Shelf Res.*, *23*, 145–157, doi:10.1016/S0278-4343(02)00190-5.

Azevedo, J. L., L. R. Oliveira, J. F. Souza, I. D. Soares, and M. M. Mata (2008), Os processos de conversão de energia nos oceanos: Uma revisão do Diagrama de Lorenz, *Braz. J. Geophys.*, *26*(2), 153–172.

Baturin, N. G., and P. P. Niiler (1997), Effects of instability waves in the mixed layer of the equatorial Pacific, *J. Geophys. Res.*, *102*, 27,771–27,793, doi:10.1029/97JC02455.

Biastoch, A., and W. Krauss (1999), The role of mesoscale eddies in the source regions of the Agulhas Current, *J. Phys. Oceanogr.*, *29*, 2303–2317, doi:10.1175/1520-0485(1999)029<2303:TROMEI>2.0.CO;2.

Bowen, M. M., J. L. Wilkin, and W. J. Emery (2005), Variability and forcing of the East Australian Current, *J. Geophys. Res.*, *110*, C03019, doi:10.1029/2004JC002533.

Brooks, I. H., and P. P. Niiler (1977), Energetics of the Florida Current, *J. Mar. Res.*, *35*, 163–191.

Brügge, B. (1995), Near-surface mean circulation and kinetic energy in the central North Atlantic from drifter data, *J. Geophys. Res.*, *100*(C10), 20,543–20,554.

Bryden, H. L. (1982), Sources of eddy energy in the Gulf Stream recirculation region, *J. Mar. Res.*, *40*, 1047–1068.

Calado, L., A. Gangopadhyay, and I. C. A. da Silveira (2006), A parametric model for the Brazil Current meanders and eddies off southeastern Brazil, *Geophys. Res. Lett.*, *33*, L12602, doi:10.1029/2006GL026092.

Campos, E. J. D., D. Velhote, and I. C. A. da Silveira (2000), Shelf break upwelling driven by Brazil Current cyclonic meanders, *Geophys. Res. Lett.*, *27*(6), 751–754, doi:10.1029/1999GL010502.

Charney, J. G. (1947), The dynamics of long waves in a baroclinic westerly current, *J. Met.*, *4*, 135–163.

Chelton, D. B., M. G. Schlax, D. L. Witter, and J. G. Richman (1990), Geosat altimeter observations of the surface circulation of the Southern Ocean, *J. Geophys. Res.*, *95*, 17,877–17,903, doi:10.1029/JC095iC10p17877.

Cheney, R. E., J. G. Marsh, and B. D. Beckley (1983), Global mesoscale variability from collinear tracks of SEASAT altimeter data, *J. Geophys. Res.*, *88*(C7), 4343–4354, doi:10.1029/JC088iC07p04343.

Cirano, M., M. M. Mata, E. J. D. Campos, and N. F. R. Deiró (2006), A circulação oceânica de larga-escala na região ao oeste do Atlântico Sul com base no modelo de circulação global OCCAM, *Rev. Bras. Geofís.*, *24*(2), 209–230.

Cronin, M., and D. R. Watts (1996), Eddy-mean flow interaction in the Gulf Stream at 68°W. Part I: Eddy energetics, *J. Phys. Oceanogr.*, *26*, 2107–2130, doi:10.1175/1520-0485(1996)026<2107:EFIITG>2.0.CO;2.

Cushman-Roisin, B. (1994), *Introduction to Geophysical Fluid Dynamics*, 320 pp., Prentice Hall, Englewood Cliffs, N. J.

de Ruijter, W. P. M., P. J. van Leeuwen, and J. R. E. Lutjeharms (1999), Generation and evolution of natal pulses: Solitary meanders in the Agulhas Current, *J. Phys. Oceanogr.*, *29*, 3043–3055, doi:10.1175/1520-0485(1999)029<3043:GAEONP>2.0.CO;2.

Dewar, W. K., and J. M. Bane (1989), Gulf Stream dynamics. Part II: Eddy energetics at 73°W, *J. Phys. Oceanogr.*, *19*, 1574–1587, doi:10.1175/1520-0485(1989)019<1574:GSDPIE>2.0.CO;2.

Emery, W. J., and R. E. Thomson (1998), *Data Analysis Methods in Physical Oceanography*, 1st ed., 634 pp., Elsevier Sci., New York.

Fratantoni, D. M. (2001), North Atlantic surface circulation during the 1990's observed with satellite-tracked drifters, *J. Geophys. Res.*, *106*(C10), 22,067–22,093, doi:10.1029/2000JC000730.

Fu, L.-L., B. Cheng, and B. Qiu (2001), 25 day period large-scale oscillations in the Argentine Basin revealed by the TOPEX/POSEIDON altimeter, *J. Phys. Oceanogr.*, *31*, 506–517, doi:10.1175/1520-0485(2001)031<0506:DPLSOI>2.0.CO;2.

Gill, A. E., J. S. A. Green, and A. J. Simmons (1974), Energy partition in the large scale ocean circulation and the production of mid-ocean eddies, *Deep Sea Res.*, *21*(7), 499–528.

Gille, S. T. (1997), The Southern Ocean momentum balance: Evidence for topographic effects from numerical model output and altimeter data, *J. Phys. Oceanogr.*, *27*, 2219–2232, doi:10.1175/1520-0485(1997)027<2219:TSOMBE>2.0.CO;2.

Goni, G., and I. Wainer (2001), Investigation of the Brazil Current front variability from altimeter data, *J. Geophys. Res.*, *106*, 31,117–31,128, doi:10.1029/2000JC000396.

Grodsky, S. A., J. A. Carton, C. Provost, J. Servain, J. A. Lorenzzetti, and M. J. McPhaden (2005), Tropical instability waves at 0°N, 23°W in the Atlantic: A case study using Pilot Research Moored Array in the Tropical Atlantic (PIRATA) mooring data, *J. Geophys. Res.*, *110*, C08010, doi:10.1029/2005JC002941.

Hall, M. M. (1991), Energetics of the Kuroshio Extension at 35°N, 152°E, *J. Phys. Oceanogr.*, *21*, 958–975, doi:10.1175/1520-0485(1991)021<0958:EOTKEA>2.0.CO;2.

Hansen, D. V., and A. Herman (1989), Temporal sampling requirements for surface drifter buoys in the tropical Pacific, *J. Atmos. Oceanic Technol.*, *6*, 599–607, doi:10.1175/1520-0426(1989)006<0599:TSRFSD>2.0.CO;2.

Hansen, D. V., and P. M. Poulin (1996), Quality control and interpolations of WOCE/TOGA drifter data, *J. Atmos. Oceanic Technol.*, *13*, 900–909, doi:10.1175/1520-0426(1996)013<0900:QCAIOW>2.0.CO;2.

Hofmann, E. E. (1985), The large-scale horizontal structure of the Antarctic Circumpolar Current from FGGE drifters, *J. Geophys. Res.*, *90*, 7080–7097.

Hogg, N. G., and W. E. Johns (1995), Western boundary currents, *Rev. Geophys.*, *33*(S1), 1311–1334, doi:10.1029/95RG00491.

Ishikawa, Y., T. Awaji, and K. Akitomo (1997), Global surface circulation and its kinetic energy distribution derived from drifting buyos, *J. Oceanogr.*, *53*, 489–516.

Kundu, P., and I. Cohen (1990), *Fluid Mechanics*, 2nd ed., 730 pp., Academic, San Diego, Calif.

Lee, D.-K., and P. P. Niiler (2005), The energetic surface circulation patterns of the Japan/East Sea, *Deep Sea Res. Part II*, *52*(11–13), 1547–1563, doi:10.1016/j.dsr2.2003.08.008.

Lee,T.N.,W.E.Johns,C.-T.Liu,D.Zang,R.Zantopp,andY.Yang(2001),(2001), (2001), Mean transport and seasonal cycle of the Kuroshio east of Taiwan with comparison to the Florida Current, *J. Geophys. Res.*, *106*(C10), 22,143–22,158, doi:10.1029/2000JC000535.

Legeckis, R., and A. L. Gordon (1982), Satellite observations of the Brazil and Falkland Currents—1975–1976 and 1978, *Deep Sea Res.*, *29*(3), 375–401, doi:10.1016/0198-0149(82)90101-7.

Lentini, A. D. C., G. J. Goni, and D. B. Olson (2006), Investigation of Brazil Current rings in the confluence region, *J. Geophys. Res.*, *111*, C06013, doi:10.1029/2005JC002988.
Mata, M. M., S. E. Wijffels, J. A. Church, and M. Tomczak (2006), Eddy shedding and energy conversions in the East Australian Current, *J. Geophys. Res.*, *111*, C09034, doi:10.1029/2006JC003592.
Matano, R. P., M. G. Schlax, and D. B. Chelton (1993), Seasonal variability in the southwestern Atlantic, *J. Geophys. Res.*, *98*, 18,027–18,035.
Morrow, R., F. Birol, D. Griffin, and J. Sudre (2004), Divergent pathways of cyclonic and anti-cyclonic ocean eddies, *Geophys. Res. Lett.*, *31*, L24311, doi:10.1029/2004GL020974.
Müller, T. J., Y. Ikeda, N. Zangenberg, and L. V. Nonato (1998), Direct measurements of western boundary currents off Brazil between 20°S and 28°S, *J. Geophys. Res.*, *103*(C3), 5429–5437, doi:10.1029/97JC03529.
Niiler, P. P. (2001), The world ocean surface circulation, in *Ocean Circulation and Climate-Observing and Modeling the Global Ocean*, edited by J. Church, G. Siedler, and J. Gould, pp. 193–204, Academic, London.
Niiler, P. P., and J. D. Paduan (1995), Wind-driven motions in the northeast Pacific as measured by Lagrangian drifters, *J. Phys. Oceanogr.*, *25*, 2819–2830, doi:10.1175/1520-0485(1995)025<2819:WDMITN>2.0.CO;2.
Nishida, H., and W. B. White (1982), Horizontal eddy fluxes of momentum and kinetic energy in the near-surface of the Kuroshio Extension, *J. Phys. Oceanogr.*, *12*, 160–170, doi:10.1175/1520-0485(1982)012<0160:HEFOMA>2.0.CO;2.
Oliveira, L. R. (2008), Energética do Atlântico Sudoeste a partir de observações lagrangeanas e de simulações do Parallel Ocean Climate Model, 226 pp., Ph.D. thesis, Univ. Fed. do Rio Grande, Rio Grande, Brazil.
Olson, D. B. (1991), Rings in the ocean, *Annu. Rev. Earth Planet. Sci.*, *19*, 283–311.
Oort, A. H., S. C. Ascher, S. Levitus, and J. P. Peixóto (1989), New estimates of the available potential energy in the World Ocean, *J. Geophys. Res.*, *94*(C3), 3187–3200, doi:10.1029/JC094iC03p03187.
Oort, A. H., L. A. Anderson, and J. P. Peixoto (1994), Estimates of the energy cycle of the oceans, *J. Geophys. Res.*, *99*, 7665–7688, doi:10.1029/93JC03556.
Orsi, A. H., T. Whitworth III, and W. D. Nowlin Jr. (1995), On the meridional extent and fronts of the Antarctic Circumpolar Current, *Deep Sea Res. Part I*, *42*, 641–673, doi:10.1016/0967-0637(95)00021-W.
Owens, W. B. (1991), A statistical description of the mean circulation and eddy variability in the northwestern North Atlantic using SOFAR floats, *Prog. Oceanogr.*, *28*, 257–303, doi:10.1016/0079-6611(91)90010-J.
Patterson, S. L. (1985), Surface circulation and kinetic energy distributions in the Southern Hemisphere oceans from FGGE drifting buoys, *J. Phys. Oceanogr.*, *15*, 865–883, doi:10.1175/1520-0485(1985)015<0865:SCAKED>2.0.CO;2.
Pedlosky, J. (1963), Baroclinic instability in two-layer systems, *Tellus*, *15*, 20–25.
Pedlosky, J. (1964), The stability of currents in the atmosphere and the oceans. Part I, *J. Atmos. Sci.*, *21*, 201–219, doi:10.1175/1520-0469(1964)021<0201:TSOCIT>2.0.CO;2.
Pedlosky, J. (1987), *Geophysical Fluid Dynamics*, 2nd ed., 710 pp., Springer, New York.
Peterson, R. G., and L. Stramma (1991), Upper-level circulation in the South Atlantic Ocean, *Prog. Oceanogr.*, *26*, 1–73, doi:10.1016/0079-6611(91)90006-8.
Phillips, H. E., and S. E. Rintoul (2000), Eddy variability and energetics from direct current measurements in the Antarctic Circumpolar Current south of Australia, *J. Phys. Oceanogr.*, *30*, 3050–3076, doi:10.1175/1520-0485(2000)030<3050:EVAEFD>2.0.CO;2.
Piola, A., H. A. Figueroa, and A. Bianchi (1987), Some aspects of the surface circulation south of 20°S revealed by first GARP Global Experiment Drifters, *J. Geophys. Res.*, *92*(C5), 5101–5114, doi:10.1029/JC092iC05p05101.
Richardson, P. L. (1983), Eddy kinetic energy in the North Atlantic Ocean from surface drifters, *J. Geophys. Res.*, *88*, 4355–4367, doi:10.1029/JC088iC07p04355.
Rossby, T. (1987), On the energetics of the Gulf stream at 73°W, *J. Mar. Res.*, *45*, 59–82, doi:10.1357/002224087788400918.
Saraceno, M., C. Provost, and A. R. Piola (2005), On the relationship of satellite retrieved surface temperature fronts and chlorophyll-a in the western South Atlantic, *J. Geophys. Res.*, *110*, C11016, doi:10.1029/2004JC002736.
Saunders, P. M., and B. A. King (1995), Bottom currents derived from shipborne ADCP on the WOCE cruise A11 in the South Atlantic, *J. Phys. Oceanogr.*, *25*, 329–347, doi:10.1175/1520-0485(1995)025<0329:BCDFAS>2.0.CO;2.
Schäfer, H., and W. Krauss (1995), Eddy statistics in the South Atlantic as derived from drifters drogued at 100 m, *J. Mar. Res.*, *53*, 403–431, doi:10.1357/0022240953213142.
Silveira, I. C. A., J. A. M. Lima, A. C. K. Schmidt, W. Ceccopieri, A. Sartori, C. P. F. Franscisco, and R. F. C. Fontes (2008), Is the meander growth in the Brazil Current system off southeast Brazil due to baroclinic instability?, *Dyn. Atmos. Oceans*, *45*, 187–207, doi:10.1016/j.dynatmoce.2008.01.002.
Stramma, L., and M. England (1999), On the water masses and mean circulation of the South Atlantic Ocean, *J. Geophys. Res.*, *104*, 20,863–20,883, doi:10.1029/1999JC900139.
Stramma, L., and R. G. Peterson (1990), The South Atlantic Current, *J. Phys. Oceanogr.*, *20*, 846–859, doi:10.1175/1520-0485(1990)020<0846:TSAC>2.0.CO;2.
Sybrandy, A. L., and P. P. Niiler (1992), The WOCE/TOGA Lagrangian drifter construction manual, *World Ocean Circ. Exp. Rep. 63/Scripps Inst. of Oceanogr. Ref. 91-6*, 58 pp., Scripps Inst. of Oceanogr., La Jolla, Calif.
Szabo, D., and G. L. Weatherly (1979), Energetics of the Kuroshio south of Japan, *J. Mar. Res.*, *37*, 531–556.
Taylor, G. I. (1922), Diffusion by continuous movement, *Proc. London Math. Soc.*, *s2-20*, 196–221, doi:10.1112/plms/s2-20.1.196.
Tisch, T. D., and S. R. Ramp (1997), Moored observations of the current and temperature structure over the continental slope off central California: 2. The energetics of the flow off Point Sur, *J. Geophys. Res.*, *102*(C10), 22,903–22,936, doi:10.1029/97JC02329.
Tomczak, M., and J. S. Godfrey (1994), *Regional Oceanography: An Introduction*, 422 pp., Pergamon, Oxford, U. K.
van Leeuwen, P. J., W. P. M. de Ruijter, and J. R. E. Lutjeharms (2000), Natal pulses and the formation of Agulhas rings, *J. Geophys. Res.*, *105*(C3), 6425–6436, doi:10.1029/1999JC900196.
Vivier, F., and C. Provost (1999), Direct velocity measurements in the Malvinas Current, *J. Geophy. Res.*, *104*(C9), 21,083–21,103.
Wilkin, J. L., and R. A. Morrow (1994), Eddy kinetic energy and momentum flux in the Southern Ocean: Comparison of a global eddy-resolving model with altimeter, drifter, and current-meter data, *J. Geophys. Res.*, *99*(C4), 7903–7916, doi:10.1029/93JC03505.
Wyrtki, K., L. Magaard, and J. Hager (1976), Eddy energy in the oceans, *J. Geophys. Res.*, *81*, 2641–2646, doi:10.1029/JC081i015p02641.

L. R. Oliveira, M. M. Mata, and I. D. Soares, Instituto de Oceanografia-Laboratório de Estudos dos Oceanos e Clima, Universidade Federal do Rio Grande, Rua Eng Alfredo Huch 475, Rio Grande RS 96201-900, Brazil. (leopoldorota@yahoo.com.br)

A. R. Piola, Servicio de Hidrografía Naval, Departamento Oceanografía, Universidad de Buenos Aires, Avenida Montes de Oca 2124, C1270ABV Buenos Aires, Argentina.